Since January 2020 Elsevier has created a COVID-19 resource centre with free information in English and Mandarin on the novel coronavirus COVID-19. The COVID-19 resource centre is hosted on Elsevier Connect, the company's public news and information website.

Biochemical and Biophysical Research Communications 567 (2021) 195–200

Contents lists available at ScienceDirect

Biochemical and Biophysical Research Communications

journal homepage: www.elsevier.com/locate/ybbrc

Optimization of reaction condition of recombinase polymerase amplification to detect SARS-CoV-2 DNA and RNA using a statistical method

Kevin Maafu Juma [a], Teisuke Takita [a], Kenji Ito [a], Masaya Yamagata [a], Shihomi Akagi [a], Emi Arikawa [a], Kenji Kojima [a, b], Manish Biyani [c, d], Shinsuke Fujiwara [e], Yukiko Nakura [f], Itaru Yanagihara [f], Kiyoshi Yasukawa [a, *]

[a] Division of Food Science and Biotechnology, Graduate School of Agriculture, Kyoto University, Kitashirakawa, Sakyo-ku, Kyoto, 606-8502, Japan
[b] Faculty of Pharmaceutical Sciences, Himeji Dokkyo University, 7-2-1 Kamiohno, Himeji, Hyogo, 670-8524, Japan
[c] Department of Bioscience and Biotechnology, Japan Advanced Institute of Science and Technology, 1-1 Asahidai, Nomi City, Ishikawa, 923-1292, Japan
[d] BioSeeds Corporation, JAIST Venture Business Laboratory, Ishikawa Create Labo 214-3, 2-13 Asahidai, Nomi City, Ishikawa, 923-1211, Japan
[e] Department of Biosciences, School of Biological and Environmental and Sciences, Kwansei-Gakuin University, 2-1 Gakuen, Sanda, Hyogo, 669-1337, Japan
[f] Department of Developmental Medicine, Research Institute, Osaka Women's and Children's Hospital, Osaka, 594-1101, Japan

ARTICLE INFO

Article history:
Received 28 May 2021
Accepted 7 June 2021
Available online 10 June 2021

Keywords:
Recombinase polymerase amplification
RPA
Recombinase
Single strand DNA-Binding protein
SARS-CoV-2
Taguchi method

ABSTRACT

Recombinase polymerase amplification (RPA) is an isothermal reaction that amplifies a target DNA sequence with a recombinase, a single-stranded DNA-binding protein (SSB), and a strand-displacing DNA polymerase. In this study, we optimized the reaction conditions of RPA to detect SARS-CoV-2 DNA and RNA using a statistical method to enhance the sensitivity. *In vitro* synthesized SARS-CoV-2 DNA and RNA were used as targets. After evaluating the concentration of each component, the uvsY, gp32, and ATP concentrations appeared to be rate-determining factors. In particular, the balance between the binding and dissociation of uvsX and DNA primer was precisely adjusted. Under the optimized condition, 60 copies of the target DNA were specifically detected. Detection of 60 copies of RNA was also achieved. Our results prove the fabrication flexibility of RPA reagents, leading to an expansion of the use of RPA in various fields.

1. Introduction

Recombinase polymerase amplification (RPA) exponentially amplifies a target nucleic acid sequence using two opposite primers at a constant temperature near 40 °C [1–3]. In RPA, recombinase binds to the primers, and the primers of the resulting complex bind to the homologous sequences of the DNA template. Then, strand-displacing DNA polymerase extends the primer, and single-stranded DNA-binding protein (SSB) binds to the unwound strand. RPA is more suitable than PCR for use in fields because it does not require a thermal cycler. Indeed, most papers on RPA published to date have been focused on detecting pathogenic organisms with amplicon-detecting technologies in consciousness of field use, such as a lateral flow assay [4], enzyme-linked oligonucleotide assay [5], and electrochemical assay [6–8].

Unlike PCR, the major limitation of RPA is that the RPA kit is sold by only two companies, Twist Dx, which is now owned by Abbott (San Diego, USA), and Jiangsu Qitian Gene Biotechnology (Ningbo, China). As a result, these RPA kits have solely been used in almost all the RPA-related studies. Such limitation makes the researchers have limited flexibility in exploring the effects of the concentration of each component on the reaction efficiency. In order to circumvent it, we previously prepared recombinant recombinase and SSB and used them to examine the effects of pH, temperature, and various additives on the efficiency of RPA [9]. In this study, we established the detection system of SARS-CoV-2 DNA and RNA and attempted to optimize the reaction condition, using one of the well-known statistical methods Taguchi method [10,11]. The results have shown that the sensitivity of RPA increased markedly by optimizing the concentration of each component.

Abbreviations: RPA, recombinase polymerase amplification; RT-RPA, reverse transcription-recombinase polymerase amplification; SSB, single-stranded DNA-binding protein; MMLV, Moloney murine leukemia virus; RT, reverse transcriptase.

* Corresponding author.
E-mail address: yasukawa.kiyoshi.7v@kyoto-u.ac.jp (K. Yasukawa).

https://doi.org/10.1016/j.bbrc.2021.06.023
0006-291X/

2. Materials and methods

2.1. Preparation of standard DNA and RNA

Standard DNA and RNA corresponding to sequences 28,571–28,970 (System 1 in Fig. 1A) and 28,171–28,470 (System 2 in Fig. 1B) of the SARS-CoV-2 gene deposited in GenBank NC_045512.2 were prepared as follows. PCR was carried out using the oligonucleotides listed in Tables S1 and S2 and *Taq* polymerase (Toyobo, Osaka, Japan) for 35 cycles of 30 s at 95 °C, 30 s at 55 °C, and 30 s at 72 °C. The amplified DNA was purified using a MagExtractor (Toyobo). *In vitro* transcription was carried out using RiboMAX Large Scale RNA Production System (Promega, Madison, WI) at 37 °C for 3 h. The synthesized RNA was purified by NICK Columns (GE Healthcare, Buckinghamshire, UK). The purified DNA and RNA concentrations were determined spectrophotometrically at A_{260}. The DNA and RNA were stored at −30 °C or −80 °C, respectively.

In System 1, the standard DNA was amplified by PCR using 400 nt_F and 400 nt_B as a pair of primers and the mixture of oligonucleotides 400nt-1, 400nt-2, and 400nt-3 as a template. The T7 promoter-bearing standard DNA was amplified by PCR using T7-400 nt_F and 400 nt_B as a pair of primers and the standard DNA as a template (Table S1). Standard RNA was synthesized by *in vitro* transcription using the T7 promoter-bearing standard DNA as a template. In System 2, the standard DNA was amplified by PCR using 300 nt_F and 300 nt_B as a pair of primes and the mixture of oligonucleotides 300nt-1 and 300nt-2 as a template. The T7 promoter-bearing standard DNA was amplified by PCR using T7-300 nt_F and 300 nt_B as a pair of primers and the standard DNA as

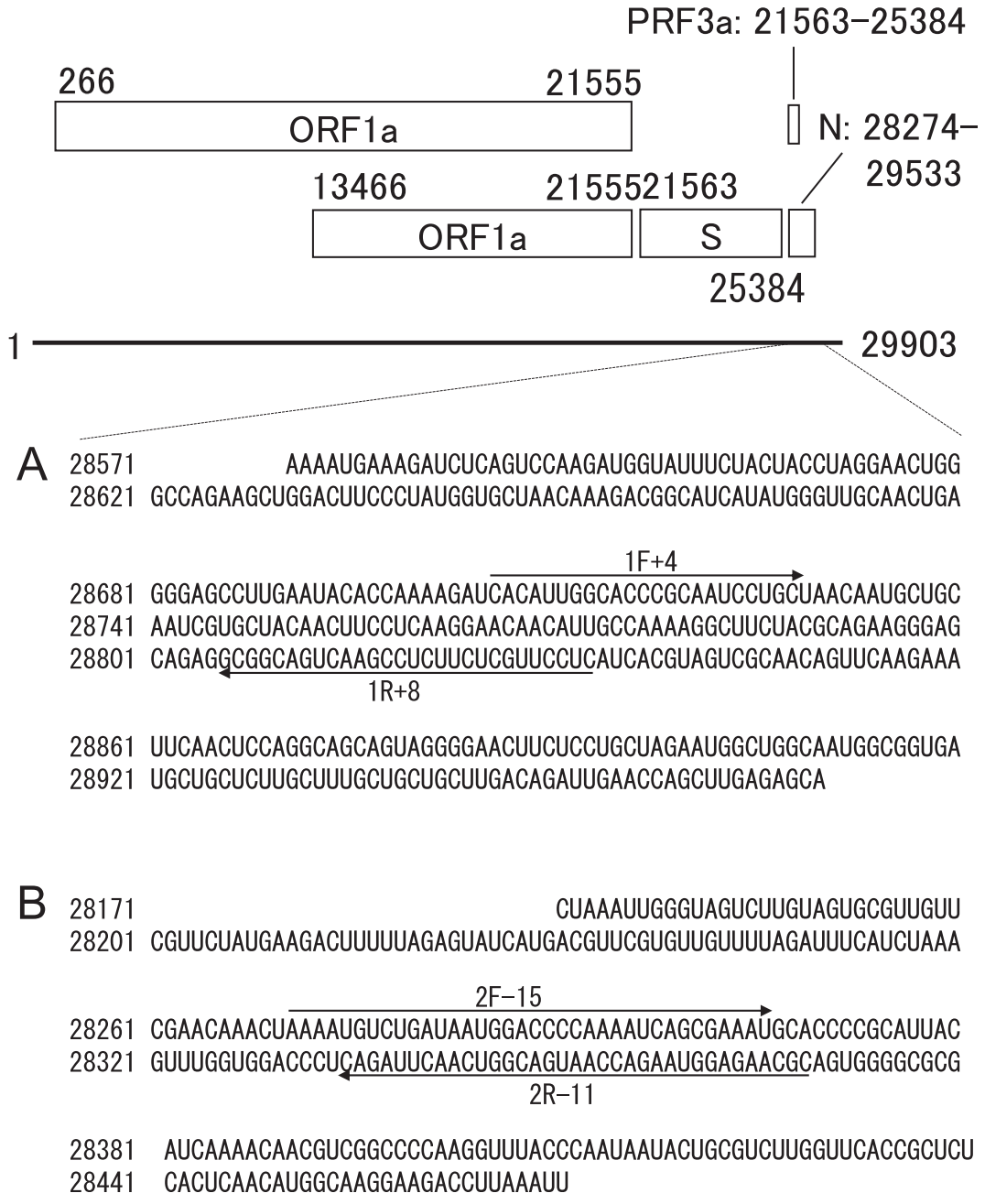

Fig. 1. Structure of SARS-CoV-2 and a target sequence for RPA amplification. Arrows indicate the sequences to which primers bind. (A) System 1. (B) System 2.

a template (Table S2). Standard RNA was synthesized by *in vitro* transcription using the T7 promoter-bearing standard DNA as a template.

2.2. Materials

Recombinant uvsX, uvsY, and gp32 were expressed in *Escherichia coli* and purified from the cells as described previously [9]. The purified uvsX, uvsY, and gp32 preparations yielded a single band with molecular masses of 43, 22, and 34 kDa, respectively (Fig. S1). *Bst* DNA polymerase (large fragment) was purchased from New England BioLabs (Ipswich, MA), and creatine kinase was purchased from Roche (Mannheim, Germany). Recombinant thermostable quadruple variant (E286R/E302K/L345R/D524A) of moloney murine leukemia virus (MMLV) reverse transcriptase (RT) was expressed in *Escherichia coli* and purified from the cells as described previously [12].

2.3. RPA reaction and statistical analysis

The reaction mixture (30 μL) for RPA was designed and prepared according to Taguchi's L27 (Table S3) orthogonal array consisting of 13 factors. The reaction was performed in a 0.2 ml PCR tube at 41 °C in PCR Thermal Cycler Dice (Takarabio, Otsu, Japan). The amplified products were separated on 2.0% (w/v) agarose gels and stained with ethidium bromide (1 μg/ml). Each reaction condition for cDNA synthesis was scored as 1, 2, or 3 according to the intensity (no, faint, or clear, respectively) of amplified products. The data were analyzed by the following equation:

$$S/N_m = -10 \log (s_m^2) \quad (1)$$

where S/N_m is signal-to-noise ratio of and s_m is the score of each reaction condition (m = 1, 2, ———, 27). The $S/N_{x,i}$ of level i (= 1, 2, or 3) of factor x (= 1 to 13) was the total of nine out of 27 S/N_m values where the level of factor x is i. For example, the $S/N_{1,1}$ and $S/N_{2,1}$ were calculated as follows:

$$S/N_{1,1} = S/N_1 + S/N_2 + S/N_3 + S/N_4 + S/N_5 + S/N_6 + S/N_7 + S/N_8 + S/N_9$$

$$S/N_{2,1} = S/N_1 + S/N_2 + S/N_3 + S/N_{10} + S/N_{11} + S/N_{12} + S/N_{19} + S/N_{20} + S/N_{21}$$

Accordingly, the lowest $S/N_{x,i}$ value of the three $S/N_{x,i}$ values ($S/N_{x,1}$, $S/N_{x,2}$, $S/N_{x,3}$) indicates that level i is the most appropriate. Variation (V_x; x = 1 to 13) and percentage contribution (P_x) for factor x were calculated using the following equations:

$$V_x = (S/N_{x,1}^2 + S/N_{x,2}^2 + S/N_{x,3}^2)/9 - (S/N_1 + S/N_2 + ——— + S/N_{27})^2/27 \quad (2)$$

$$P_x = V_x / (V_1 + V_2 + ——— + V_{13}) \times 100 \quad (3)$$

Accordingly, high V_x and P_x values indicate that the effect of the difference in the three levels in factor x is high on the reaction efficiency.

3. Results and discussion

3.1. Establishment of the RPA detection systems of SARS-CoV-2 DNA

For use as the assay in the optimization of RPA reaction condition, we established a detection system (System 1) of SARS-CoV-2 DNA (Fig. 1A). In System 1, nucleocapsid phosphoprotein gene was selected as a target according to the previous report [13]. We designed three forward and three reverse primers (Table S1), and selected one combination (1F+4 and 1R+8) that exhibited the best performance in sensitivity. The size of amplified product by the primer combination was 128 bp.

3.2. Round 1 of optimization of RPA reaction condition

We designed 13 factors and three concentrations (levels 1–3) for each factor (Table S4). Level 2 was set as the concentration used in the standard condition with which we previously examined the effects of pH, CH_3COOK concentration, and temperature on the RPA reaction efficiency [9]. Levels 1 and 3 were set as 25–50% and 200–400%, respectively, of level 2. According to Taguchi's L27 orthogonal array (Table S3), the RPA reaction was carried out with 6×10^8 copies (2×10^7 copies/μL) of standard DNA and primers in System 1. The reaction products at 30, 45, and 60 min was analyzed by agarose gel electrophoresis. As an example, one of the results is shown in Fig. S2. Of the 27 reaction conditions, six (2, 3, 7, 17, 24, and 25) exhibited clear, four (5, 12, 13, and 18) exhibited faint, and the other 17 exhibited no 128-bp band corresponding to the amplified product. The signal-to-noise ratios for each reaction condition (S/N_m; m = 1 to 27), those for each level of each factor ($S/N_{x,i}$; x = 1 to 13, i = 1, 2, or 3), and variations (V) and percentage contributions (P) for each factor were calculated (Table S4). The results indicated that the $Mg(OCOCH_3)_2$ concentration exhibited the highest V (142) and P (39.7%) values with the optimal concentration of 7 mM (level 1).

It is known that the optimal concentration of $Mg(OCOCH_3)_2$ depends on primer and target sequences. Indeed, in the RPA kit sold by Twist Dx, $Mg(OCOCH_3)_2$ is not premixed but is added by users. High V and P values in our results suggested that the optimal range of $Mg(OCOCH_3)_2$ concentration is relatively narrow.

3.3. Rounds 2 and 3 of optimization of RPA reaction condition

The 13 factors and each three levels in Round 2 are shown in Table S5. Based on the results of Round 1 where the $Mg(OCOCH_3)_2$ concentrations were set as 7, 14, and 28 mM, for levels 1, 2, and 3, respectively, they were set as 5, 8, and 11 mM in Round 2. The concentrations of PEG35000, dNTPs, ATP, and primers were also altered. Tris-HCl (pH 8.2) was replaced with phosphocreatine. Twenty-seven RPA reactions were carried out with 6×10^8 copies (2×10^7 copies/μL) of standard DNA and primers in System 1. Results are shown in Table S5, indicating that the optimal uvsY, gp32, and ATP concentrations were not level 2 but level 1 (35 ng/μL) for uvsY, level 3 (400 ng/μL) for gp32, and level 1 (3 mM) for ATP concentrations. In addition, the uvsX, uvsY, gp32, and ATP concentrations exhibited relatively high V (21.1, 35.3, 130.4, and 28.6, respectively) and P values (4.2%, 6.9%, 25.7%, and 5.6%, respectively). These results suggested that these concentrations were rate-determining factors.

In the RPA process, the balance of the binding and dissociation between uvsX and DNA primer is important. In the presence of ATP, uvsX binds to DNA primer to form the nucleoprotein with the aid of uvsY. Upon hydrolysis of ATP, uvsX dissociates from DNA primer and is replaced by gp32. Thus, uvsX, uvsY, and ATP shift the balance to the binding, while gp32 shifts it to the dissociation. If this binding affinity is not high enough, the nucleoprotein cannot invade double-stranded DNA, thereby preventing DNA primer from binding to the target sequence. On the other hand, if the binding affinity is too high, uvsX remains occupied even after the elongation starts, preventing another nucleoprotein from binding to the target sequence and starting the elongation. Therefore, it was thought that the binding affinity of the reaction condition

consisting of level 2 for all 13 factors' concentrations was too high.

Based on the results of Round 2, we attempted to lower the binding affinity by increasing the concentration of gp32 and decreasing the concentrations of uvsY and ATP. Thirteen factors and each three levels in Round 3 were determined (Table S6). Twenty-seven RPA reactions were carried out with 6×10^4 copies (2×10^3 copies/μL) of standard DNA and primers using System 1. Results are shown in Table S6. Level 2 was optimal for the uvsX and gp32 concentrations. The uvsY concentration exhibited low V (12.6) and P (3.9%) values. These results suggested that the balance between the binding and dissociation of uvsX and DNA primer was adequately adjusted.

3.4. Performance of the optimized reaction condition

For use as the assay in the optimization of RPA reaction condition, we established two detection systems (Systems 1 and 2) of SARS-CoV-2 DNA and RNA (Fig. 1B). In System 2, ORF8 protein gene was used as a target because Centers for Disease Control and Prevention (CDC), USA reported the PCR primers targeting this region, and these primers are widely used in approved diagnostics of SARS-CoV-2 RNA. We designed nine forward and eight reverse primers (Table S2) and selected one combination (2F-15 and 2R-11) that exhibited the best performance in sensitivity. The size of amplified product by the primer combination was 99 bp.

RPA was carried out with 60–6×10^7 copies of standard DNA, and RT-RPA was carried out with 60–6×10^7 copies of standard RNA, both at 41 °C for 1 h. In the analysis of the RPA or RT-RPA products in the subsequent electrophoresis, the optimized conditions detected 60 copies of standard DNA (Fig. 2A) or RNA (Fig. 2B).

Finally, we compared the sensitivities of RPA before and after optimization. Using System 2, RPA was carried out with 60–6×10^7 copies of standard DNA (Fig. S3). The condition after optimization detected 60 copies of standard DNA while that before optimization did not detect 600 copies. These results indicated that by optimizing the reaction conditions for three enzymes, 100 to 1000-fold higher sensitivity was achieved.

Generally, the performance of a nucleic acid amplification test depends largely on the performance of the enzymes involved. Indeed, DNA polymerases and RTs whose activity and/or stability have been improved by genetic engineering technique are currently used in PCR and RT-PCR [14,15]. However, such improvement has not been done for recombinase and SSB. It is of note that the optimal concentrations of uvsX, uvsY, and gp32 in the RPA reaction solution are in the range of 1–10 μM, which is 1000-fold higher than reverse transcriptase and thermostable DNA polymerase in cDNA synthesis and PCR. Such high protein concentration makes RPA reagents less flexible in fabrication. To solve this problem, increase in activity and/or binding ability of recombinase and SSB is required. On the other hand, considering the filed use of RPA, it is anticipated that storage of the reagents at room temperature is possible. To address this issue, use of thermostable recombinase and SSB from thermophilic organisms might be useful.

In PCR, various additives that increase the reaction efficiency have been reported: bovine serum albumin, trehalose, sorbitol, glycerol, Triton X-100, and Tween 20 stabilize an enzyme, and dimethyl sulfoxide, formamide, and ammonium sulfate increase specificity [16,17]. Helicase increases specificity by decreasing non-specific binding [18]. Spermidine suppresses reaction inhibition problems encountered while analyzing clinical stool samples [19,20]. In RPA, little is known for such additives except for the recent report that betaine increases specificity [21]. Our results in this study might make the evaluation of the effects of various additives on the RPA reaction efficiency easier.

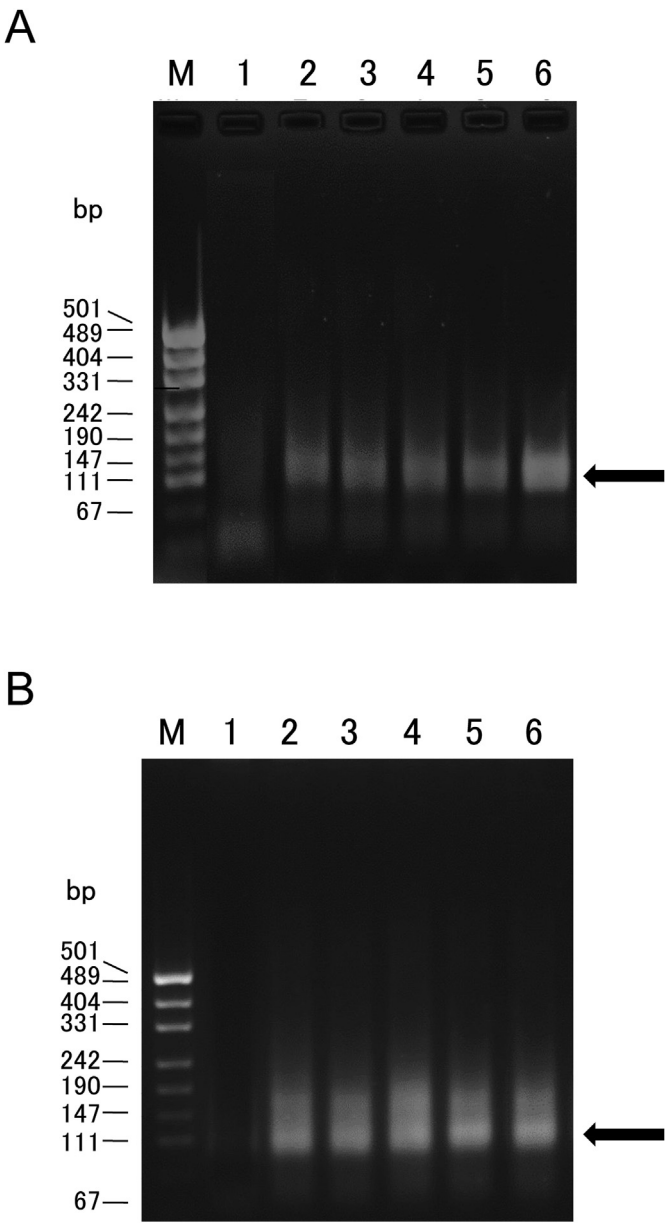

Fig. 2. Comparison of the sensitivities of RPA and RT-RPA. (A) RPA. (B) RT-RPA. The reactions (30 μL) were carried out with 400 ng/μL uvsX, 40 ng/μL uvsY, 400 ng/μL gp32, 0.4 units/μL *Bst* DNA polymerase, 120 ng/μL creatine kinase, 2 mM DTT, 6% PEG35000, 3.5 mM ATP, 650 μM dNTPs, 3.5 mM ATP, 50 mM Tris-HCl buffer (pH 8.6), 40 mM CH_3COOK, 20 mM phosphocreatine, 8 mM $Mg(OCOCH_3)_2$, 1 μM 2F-15 primer, and 1 μM 2R-11 primer in the absence (A) or presence (B) of 100 nM MMLV RT, at 41 °C for 30 min. Initial copies of standard DNA (A) and RNA (B): 0 (lane 1), 60 (lane 2), 600 (lane 3), 6×10^3 (lane 4), 6×10^5 (lane 5), and 6×10^7 (lane 6). Black arrow indicates the 99-bp target band.

3.5. Insights into the effect of the balance between the binding and dissociation of uvsX and DNA primer on the RPA reaction efficiency

As described above, Round 2 revealed that the reaction efficiency of RPA depends on the balance of the binding and dissociation between uvsX and DNA primer. To further understand this issue, we examined the effects of the concentrations of uvsX, uvsY, gp32, and ATP on RPA efficiency. The optimized condition obtained by Round 4 were used as standard conditions. Fig. 3 shows the analysis of the RPA products at 30 min using agarose gel electrophoresis. An amplified DNA band was observed at 400–4000 ng/μL

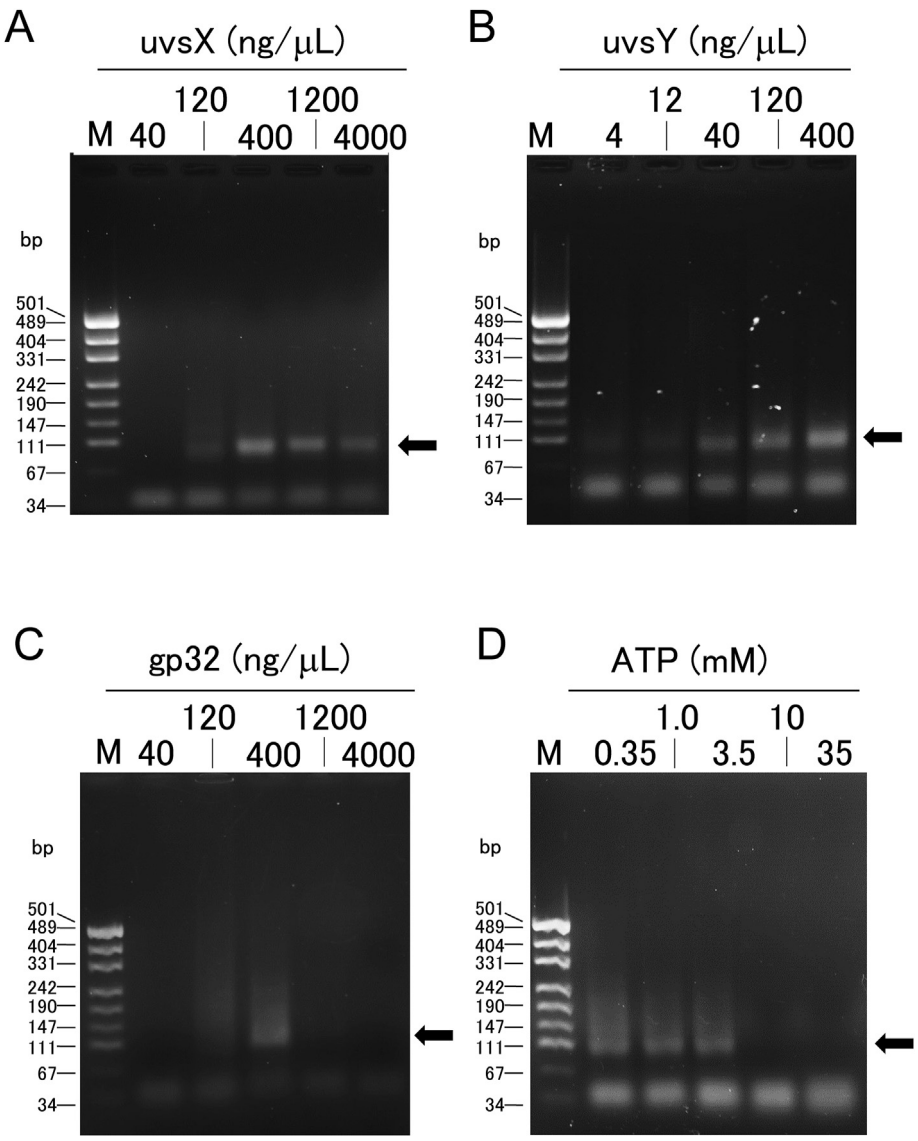

Fig. 3. Effects of the concentrations of uvsX, uvsY, gp32, and ATP on the reaction efficiency of RPA. (A–D) The reactions (30 μL) were carried out with 40–4000 (A) or 400 (B–D) ng/μL uvsX, 4–400 (B) or 40 (A, C, D) ng/μL uvsY, 40–4000 (C) or 400 (A, B, D) ng/μL gp32, 0.4 units/μL *Bst* DNA polymerase, 120 ng/μL creatine kinase, 2 mM DTT, 6% PEG35000, 0.35–35 (D) or 3.5 (A–C) mM ATP, 650 μM dNTPs, 50 mM Tris-HCl buffer (pH 8.6), 40 mM CH_3COOK, 20 mM phosphocreatine, 8 mM $Mg(OCOCH_3)_2$, 1 μM 2F-15 primer, and 1 μM 2R-11 primer at 41 °C for 30 min. Initial copies of standard DNA was 6000. The arrow indicates the 99-bp target band.

uvsX, 40–400 ng/μL uvsY, 400 ng/μL gp32, and 0.35–3.5 mM ATP, while it was not observed at 40 and 120 ng/uL uvsX, 4 and 12 ng/μL uvsY, 40, 120, 1200, and 4000 ng/μL gp32, or 10 and 35 mM ATP. These results indicated that the optimal concentration of gp32 is narrower than that of uvsX, uvsY, and ATP, suggesting that the gp32 concentration is critical for the balance of the binding and dissociation between uvsX and DNA primer.

It is known that uvsX, uvsY, and gp32 form a ternary complex with a single-stranded DNA (ssDNA) [22]. Gajewski et al. performed the crystal structural analysis of the uvsY-ssDNA complex and showed that uvsX exists as a heptamer [23]. They also provided a model showing that uvsY promotes a helical ssDNA conformation that disfavors the binding of gp32 and initiates the assembly of the ssDNA–uvsX filament [23]. We presume that this model might be applicable to the mechanism of RPA reaction.

In conclusion, the sensitivity of RPA and RT-RPA for SARS-CoV-2 DNA and RNA increased by optimizing the concentration of each component using a statistical method. Our results pave the way for use of RPA in various fabrications.

Notes

The authors declare no competing financial interest.

Acknowledgments

We acknowledge Ms. Mika Ishitani for her technical assistance. This work was supported in part by SENTAN (S.F., I.Y., K.Y.) from Japan Science and Technology Agency, Grants-in-Aid for Scientific Research (no. 18KK0285 for K.K., T.T., and K.Y., and 18K19839 for M.B., K.Y.) from Japan Society for the Promotion of Science, Emerging/re-emerging infectious disease project of Japan (grant no. 20he0622020h0001 for M.B., S.F., I.Y., K.Y. and grant no. 20fk0108143h001 for S.F., I.Y., K.Y.) from Japan Agency for Medical Research and Development, and Grant Program for Biomedical Engineering Research (grant no. 2018T006 for S.F., I.Y., K.Y.) from Nakatani Foundation, Japan.

Appendix A. Supplementary data

Supplementary data to this article can be found online at https://doi.org/10.1016/j.bbrc.2021.06.023.

References

[1] O. Piepenburg, C.H. Williams, D.L. Stemple, N.A. Armes, DNA detection using recombination proteins, PLoS Biol. 4 (2006), e204, https://doi.org/10.1371/journal.pbio.0040204.

[2] I.M. Lobato, C.K. O'Sullivan, Recombinase polymerase amplification: basics, applications and recent advances, Trends Anal. Chem. 98 (2018) 19–35.

[3] J. Li, J. Macdonald, F. von Stetten, Review: a comprehensive summary of a decade development of the recombinase polymerase amplification, Analyst 144 (2019) 31–67, https://doi.org/10.1016/j.trac.2017.10.015.

[4] M. Jauset-Rubio, H. Tomaso, M.S. El-Shahawi, A.S. Bashammakh, A.O. Al-Youbi, C.K. O'Sullivan, Duplex lateral flow assay for the simultaneous detection of *Yersinia pestis* and *Francisella tularensis*, Anal. Chem. 90 (2018) 12745–12751, https://doi.org/10.1021/acs.analchem.8b03105.

[5] A. Toldrà, M. Jauset-Rubio, K.B. Andree, M. Fernández-Tejedor, J. Diogène, I. Katakis, C.K. O'Sullivan, M. Campàs, Detection and quantification of the toxic marine microalgae *karlodinium veneficum* and *karlodinium armiger* using recombinase polymerase amplification and enzyme-linked oligonucleotide assay, Anal. Chim. Acta 1039 (2018) 140–148, https://doi.org/10.1016/j.aca.2018.07.057.

[6] S. Al-Madhagi, H. Joda, M. Jauset-Rubio, M. Ortiz, I. Katakis, C.K. O'Sullivan, Isothermal amplification using modified primers for rapid electrochemical analysis of coeliac disease associated DQB1*02 HLA allele, Anal. Biochem. 556 (2018) 16–22, https://doi.org/10.1016/j.ab.2018.06.013.

[7] J. Sabaté del Río, T. Steylaerts, O.Y.F. Henry, P. Bienstman, T. Stakenborg, W.V. Roy, C.K. O'Sullivan, Real-time and label-free ring-resonator monitoring of solid-phase recombinase polymerase amplification, Biosens. Bioelectron. 73 (2015) 130–137, https://doi.org/10.1016/j.bios.2015.05.063.

[8] H. Rathore, R. Biyani, H. Kato, Y. Takamura, M. Biyani, Palm-size and one-inch gel electrophoretic device for reliable and field-applicable analysis of recombinase polymerase amplification, Anal. Methods 11 (2019) 4953–5072, https://doi.org/10.1039/C9AY01476D.

[9] K. Kojima, K.M. Juma, S. Akagi, K. Hayashi, T. Takita, C.K. O'Sullivan, S. Fujiwara, Y. Nakura, I. Yanagihara, K. Yasukawa, Solvent engineering studies on recombinase polymerase amplification, J. Biosci. Bioeng. 131 (2021) 219–224, https://doi.org/10.1016/j.jbiosc.2020.10.001.

[10] P. Thanakiatkrai, L. Welc, Using the Taguchi method for rapid quantitative PCR optimization with SYBR Green I, Int. J. Leg. Med. 126 (2012) 161–165, https://doi.org/10.1007/s00414-011-0558-5.

[11] H. Okano, Y. Katano, M. Baba, A. Fujiwara, R. Hidese, S. Fujiwara, I. Yanagihara, T. Hayashi, K. Kojima, T. Takita, K. Yasukawa, Enhanced detection of RNA by MMLV reverse transcriptase coupled with thermostable DNA polymerase and DNA/RNA helicase, Enzym. Microb. Technol. 96 (2017) 111–120, https://doi.org/10.1016/j.enzmictec.2016.10.003.

[12] K. Yasukawa, M. Mizuno, A. Konishi, K. Inouye, Increase in thermal stability of Moloney murine leukaemia virus reverse transcriptase by site-directed mutagenesis, J. Biotechnol. 150 (2010) 299–306, https://doi.org/10.1016/j.jbiotec.2010.09.961.

[13] V.M. Corman, O. Landt, M. Kaiser, R. Molenkamp, A. Meijer, D.K. Chu, T. Bleicker, S. Brünink, J. Schneider, M.L. Schmidt, D.Q. Mulders, B.L. Haagmans, B. van der Veer, S. van den Brink, L. Wijsman, G. Goderski, J.I. Romette, J. Ellis, M. Zambon, M. Peiris, H. Goossens, C. Reusken, M.P. Koopmans, C. Drosten, Detection of 2019 novel coronavirus (2019-nCoV) by real-time RT-PCR, Euro Surveill. 25 (2020) 2000045, https://doi.org/10.2807/1560-7917.ES.2020.25.3.2000045.

[14] Y. Ishino, Studies on DNA-related enzymes to elucidate molecular mechanisms underlying genetic information processing and their application in genetic engineering, Biosci. Biotechnol. Biochem. 84 (2020) 1749–1766, https://doi.org/10.1080/09168451.2020.1778441.

[15] K. Yasukawa, I. Yanagihara, S. Fujiwara, Alteration of enzymes and their application to nucleic acid amplification (Review), Int. J. Mol. Med. 46 (2020) 1633–1643, https://doi.org/10.3892/ijmm.2020.4726.

[16] H. Grunenwald, Optimization of polymerase chain reactions, in: J.M.S. Bartlett, D. Stirling (Eds.), PCR Protocols, second ed., Humana Press, Totowa, 2003, pp. 89–99, 89, https://link.springer.com/protocol/10.1385/1-59259-384-4.

[17] A.N. Spiess, N. Mueller, R. Ivell, Trehalose is a potent PCR enhancer: lowering of DNA melting temperature and thermal stabilization of taq polymerase by the disaccharide trehalose, Clin. Chem. 50 (2004) 1256–1259, https://doi.org/10.1373/clinchem.2004.031336.

[18] R. Hidese, K. Kawato, Y. Nakura, A. Fujiwara, K. Yasukawa, I. Yanagihara, S. Fujiwara, Thermostable DNA helicase improves the sensitivity of digital PCR, Biochem. Biophys. Res. Commun. 495 (2018) 2189–2194, https://doi.org/10.1016/j.bbrc.2017.12.053.

[19] J.P. Roperch, K. Benzekri, H. Mansour, R. Incitti, Improved amplification efficiency on stool samples by addition of spermidine and its use for non-invasive detection of colorectal cancer, BMC Biotechnol. 15 (2015) 41, https://doi.org/10.1186/s12896-015-0148-6.

[20] A. Kikuchi, T. Sawamura, N. Kawase, Y. Kitajima, T. Yoshida, O. Daimaru, Y. Nakakita, S. Itoh, Utility of spermidine in PCR amplification of stool samples, Biochem. Genet. 48 (2010) 428–432, https://doi.org/10.1007/s10528-009-9326-3.

[21] G.C. Luo, T.T. Yi, B. Jiang, X.L. Guo, G.Y. Zhang, Betaine-assisted recombinase polymerase assay with enhanced specificity, Anal. Biochem. 575 (2019) 36–39, https://doi.org/10.1016/j.ab.2019.03.018.

[22] K. Hashimoto, T. Yonesaki, The characterization of a complex of three bacteriophage T4 recombination proteins, uvsX protein, uvsY protein, and gene 32 protein, on single-stranded DNA, J. Biol. Chem. 266 (1991) 4883–4888, https://doi.org/10.1016/S0021-9258(19)67731-8.

[23] S. Gajewski, M.B. Waddell, S. Vaithiyalingam, A. Nourse, Z. Li, N. Woetzel, N. Alexander, J. Meiler, S.W. White, Structure and mechanism of the phage T4 recombination mediator protein UvsY, Proc. Natl. Acad. Sci. U.S.A. 113 (2016) 3275–3280, https://doi.org/10.1073/pnas.1519154113.